

## Stability Analysis of Stagnation-Point Flow and Heat Transfer over an Exponentially Shrinking Sheet with Heat Generation

Ismail, N. S. <sup>\*1</sup>, Arifin, N. M. <sup>1,2</sup>, Nazar, R. <sup>3</sup>, and Bachok, N. <sup>1,2</sup>

<sup>1</sup>*Institute for Mathematical Research, Universiti Putra Malaysia, Malaysia*

<sup>2</sup>*Department of Mathematics, Faculty of Science, Universiti Putra Malaysia, Malaysia*

<sup>3</sup>*School of Mathematical Sciences, Faculty of Science and Technology, Universiti Kebangsaan Malaysia, Malaysia*

*E-mail: syuhada.polaris@gmail.com*

*\* Corresponding author*

*Received: 9 October 2017*

*Accepted: 27 March 2019*

### ABSTRACT

This case study seeks to examine the fluid flow at stagnation-point over an exponentially permeable shrinking sheet towards suction. This work also investigate the heat transfer in the present of heat generation. By using an appropriate similarity transformation, we obtain ordinary differential equations by reduction of governing partial differential equation. We used commercially Maple software to obtain the numerical result. The effects of the parameters involve in this study are summarizes and thoroughly discussed. Remarkably, the dual solution is found at certain range of the shrinking sheet and suction parameters. Thus, this result is further performed to analyze its stability by using Matlab software. As expected, our study has proved that the first solution is stable while the second one is not.

**Keywords:** Heat generation, exponentially, Stability analysis, Shrinking sheet, Stagnation point, Suction.

## 1. Introduction

Research on heat transfer problems is important to the applications in industries and engineering such as automotive engineering, power station engineering, materials processing, thermal management of electronic devices and systems. Heat transfer strongly depends on the fluid velocity, fluid properties, geometry, type of fluid flow and coarseness of the solid surface. A good quality of the final product can be obtained by using the shrinking surface which is one of the applications used in controlling the rate of heat transfers. A number of authors have reported that dual solutions can exist in shrinking sheet problems. Preliminary work to obtain non-unique solutions in shrinking sheet problem was undertaken by Miklavcic and Wang (2006). Different authors have studied the shrinking sheet problem in a variety of ways such as Wang (2008), Fang (2008), Fang and Zhang (2009), Bhattacharyya (2011), Bachok et al. (2012), Saleh et al. (2014), Bhatti and Rashidi (2016) and Khan et al. (2017). The stagnation flow (which contains the vorticity) against a shrinking sheet was first published by Wang (2008). At the surface of the object in the flow field, there are existences of stagnation points when the fluid appears to rest effected from the object. The problems on stagnation point which can be viewed in the literature have been considered by Mahapatra et al. (2010), Mahapatra and Nandy (2011), Bhattacharyya and Vajravelu (2012), Bachok et al. (2012) and others. Bhattacharyya (2011) was the first who studied the problem of the exponentially shrinking sheet and several other studies later on can be found in Bhattacharyya and Vajravelu (2012), Bachok et al. (2012), Rohni et al. (2013), Hsiao (2016) and Naveed et al. (2017).

On the other hand, free convection is driven by internal heat generation is one of the physical phenomena commonly occurs. Heat generation is referred to as the convection of some form of energy into sensible heat energy in the medium. Examples of the energy are electrical, chemical and nuclear energy. Heat generation occurs throughout the medium and exhibits itself as a rise in temperature. One study by Molla et al. (2006) examined the fluid flow in natural convection with influence of heat generation. They come to the conclusion that, the increment of heat generation parameter tends the skin friction coefficient increase while the Nusselt number decrease and this results consistent with works by Malvandi et al. (2013). In addition, the applying of suction is also important in various engineering applications such as in chemical processes to remove reactants. In general, the presence of suction have a tendency

to increase the skin friction. There are some papers reported by Elbashbeshy and Bazid (2004) and El-Bashbeshy et al. (2015) about both parameters of suction and heat generation that have uniform results. They have concluded that, the increment of heat generation parameter tends the increasing of skin friction coefficient meanwhile the decreasing of Nusselt number. Furthermore, the heat transfer rate is increasing as the suction parameter increase. This has also been explored by Nandy and Mahapatra (2013), Suriyakumar and Devi (2015), Gireesha et al. (2016), Animasaun et al. (2016) and Rashad et al. (2017),

The stability analysis is roughly connected with numerical errors. If the errors produced at the first step of the calculation does not create the errors as the computations continue, the finite difference scheme is stable. On the other hand, if the error grows with time while the computations continue, the numerical scheme will be unstable. Stability analysis is undergoing a generating considerable interest in the field of fluid dynamics since non unique solutions is reported. Some of the papers include an early work by Merkin (1986) and other papers by Weidman et al. (2006), Roşca and Pop (2013), Ishak (2014), Sharma et al. (2014), Hafidzuddin et al. (2015), Awaludin et al. (2016) and Jahan et al. (2017). This research provides a framework for the exploration of the fluid flow by extended paper by Bhattacharyya and Vajravelu (2012) with added the effects of suction and heat generation.

## 2. Mathematical Formulation

Before considering the governing equations to this study, it is important to note some assumption for build the appropriate equations. First, let us consider a steady and two-dimensional stagnation-point flow over an exponentially permeable shrinking sheet of an incompressible viscous fluid in the presence of heat generation. The shrinking/stretching sheet velocity is  $U_w$ , straining velocity is  $U_e$ ,  $T_w$  is the temperature at the surface and  $T_\infty$  is the temperature at surrounding where it is assumed to be constant. Figure 1 illustrates the flow configuration of this problem.

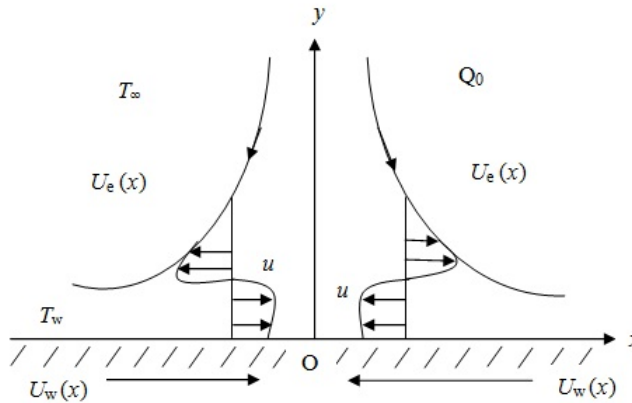


Figure 1: A sketch of physical model and coordinate system

Under the assumptions, the governing equations for the current study are (Bhattacharyya and Vajravelu (2012))

$$\frac{\partial u}{\partial x} + \frac{\partial v}{\partial y} = 0 \quad (1)$$

$$u \frac{\partial u}{\partial x} + v \frac{\partial u}{\partial y} = U_e \frac{\partial U_e}{\partial x} + \nu \frac{\partial^2 u}{\partial y^2} \quad (2)$$

$$u \frac{\partial T}{\partial x} + v \frac{\partial T}{\partial y} = \alpha \frac{\partial^2 T}{\partial y^2} + \frac{Q_0}{\rho c_p} (T - T_\infty) \quad (3)$$

with the conditions at the boundary are

$$\begin{aligned} u = U_w(x), \quad v = v_w, \quad T = T_w = T_\infty + T_0 \exp\left(\frac{x}{2L}\right) \quad \text{at } y = 0, \\ u \rightarrow U_e(x), \quad T \rightarrow T_\infty \quad \text{as } y \rightarrow \infty \end{aligned} \quad (4)$$

where the velocity components in the  $x$  direction is  $u$  and  $y$  direction is  $v$ . The shrinking/stretching velocity is  $U_w(x) = c \exp(\frac{x}{L})$ , the straining velocity is  $U_e(x) = a \exp(\frac{x}{L})$ ,  $\nu$  is the kinematic viscosity,  $\alpha$  is the thermal diffusivity,  $\rho$  is the fluid density,  $v_w$  is the mass transfer velocity,  $c_p$  is the specific heat,  $L$  is the characteristic length of the sheet,  $c$  is the shrinking/stretching velocity rate where  $c < 0$  for shrinking sheet and  $c > 0$  for stretching sheet,  $a > 0$  is the straining velocity rate and  $Q_0$  is the dimensional heat generation coefficient. Similarity solution of (1) - (4) can be obtain by apply the following similarity transformations:

$$\psi = \sqrt{2\nu La} f(\eta) \left( \frac{x}{2L} \right), \quad T = T_\infty + (T_w - T_\infty) \theta(\eta)$$

$$\eta = y \sqrt{\frac{a}{2\nu L}} \exp \left( \frac{x}{2L} \right) \quad (5)$$

where  $\psi$  and  $\eta$  are the stream function and similarity variable, respectively. The stream function is always be denoted as  $u = \partial\psi/\partial y$  and  $v = -\partial\psi/\partial x$ . Hence, we obtain

$$u = U_e(x) f'(\eta), \quad v = -\sqrt{\frac{\nu a}{2L}} \exp \left( \frac{x}{2L} \right) [f(\eta) + \eta f'(\eta)]$$

$$v_w = -\sqrt{\frac{\nu a}{2L}} \exp \left( \frac{x}{2L} \right) s \quad (6)$$

where we defined the dimensionless suction parameter as  $s > 0$ . Then, substitute equation (5) and (6) into equations (2) and (3), we obtained the ODEs as below:

$$f''' + f f'' + 2(1 - f'^2) = 0, \quad (7)$$

$$\frac{1}{Pr} \theta'' + f \theta' - f' \theta + Q \theta = 0, \quad (8)$$

and the boundary conditions (4) transform to

$$f(\eta) = s, \quad f'(\eta) = \lambda, \quad \theta(\eta) = 1 \quad \text{at} \quad \eta = 0$$

$$f'(\eta) \rightarrow 1, \quad \theta(\eta) \rightarrow 0 \quad \text{as} \quad \eta \rightarrow \infty \quad (9)$$

where  $Pr$  is the Prandtl number with  $Pr = \mu c_p / \kappa$ ,  $Q$  is the heat generation parameter and  $\lambda = c/a$  is the stretching/shrinking parameter. Next, the skin-friction coefficient  $C_f$  and the Nusselt number  $Nu$  is always to be physical quantities of interest in this research which can respectively be written as

$$C_f = \frac{\tau_w}{\rho U_e^2}, \quad Nu = \frac{q_w}{(T_w - T_\infty)} \quad (10)$$

where  $\tau_w$  and  $q_w$  are wall shear stress and local heat flux, respectively which are declares as

$$\tau_w = \mu \left( \frac{\partial u}{\partial y} \right)_{y=0}, \quad q_w = \left( -\frac{\partial T}{\partial y} \right)_{y=0} \quad (11)$$

After that, substituting (5) into equations (10) and (11), we get

$$\sqrt{2ReC_f} = f''(0), \quad \text{and} \quad \sqrt{2/ReNu} = -\theta'(0) \quad (12)$$

where  $Re = U_e L / \nu$  is the Reynolds number.

### 3. Stability Analysis

To allow us to perform a stability analysis, the primary step is the steady problem will consider an unsteady problem. Thus, we introduce the new dimensionless variable for the unsteady problem based on the variables (5) previously

$$\begin{aligned} \psi &= \sqrt{2\nu L a} \exp\left(\frac{x}{2L}\right) f(\eta, \tau), \quad T = T_\infty + (T_w - T_\infty)\theta(\eta, \tau), \\ \eta &= y \sqrt{\frac{a}{2\nu L}} \exp\left(\frac{x}{2L}\right), \quad \tau = \frac{a \exp^{x/L} t}{2L} \end{aligned} \quad (13)$$

Thus, the equation (2) and (3) change to the following equation

$$\frac{\partial^3 f}{\partial \eta^3} + f \frac{\partial^2 f}{\partial \eta^2} - 2 \left(\frac{\partial f}{\partial \eta}\right)^2 + 2 - \frac{\partial^2 f}{\partial \eta \partial \tau} - 2\tau \frac{\partial f}{\partial \eta} \frac{\partial^2 f}{\partial \eta \partial \tau} - 2\tau \frac{\partial^2 f}{\partial \eta^2} \frac{\partial f}{\partial \tau} = 0, \quad (14)$$

$$\frac{1}{Pr} \frac{\partial^2 \theta}{\partial \eta^2} + f \frac{\partial \theta}{\partial \eta} - \frac{\partial f}{\partial \eta} \theta + Q\theta - \frac{\partial \theta}{\partial \tau} - 2\tau \frac{\partial \theta}{\partial \tau} \frac{\partial f}{\partial \eta} - 2\tau \frac{\partial \theta}{\partial \eta} \frac{\partial f}{\partial \tau} = 0 \quad (15)$$

and also the boundary conditions (4) change to

$$\begin{aligned} f(\eta, \tau) = s, \quad \frac{\partial f}{\partial \eta}(\eta, \tau) = \lambda, \quad \theta(\eta, \tau) = 1 \quad \text{at} \quad \eta = 0, \\ \frac{\partial f}{\partial \eta}(\eta, \tau) \rightarrow 1, \quad \theta(\eta, \tau) \rightarrow 0 \quad \text{as} \quad \eta \rightarrow \infty \end{aligned} \quad (16)$$

where t denotes the time. To enable us to test the stability of the solutions, we introduce the following equations (Ishak (2014))

$$\begin{aligned} f(\eta, \tau) &= f_0(\eta) + e^{-\gamma\tau} F(\eta), \\ \theta(\eta, \tau) &= \theta_0(\eta) + e^{-\gamma\tau} G(\eta), \end{aligned} \quad (17)$$

where  $F(\eta, \tau)$  small relative to  $f_0(\eta)$ ,  $G(\eta, \tau)$  small relative to  $\theta_0(\eta)$  and  $\gamma$  is an unknown eigenvalue. Next, differentiate equation (17) and then substitute into equation (14) and (15) to obtain the eigenvalue problem as below

$$F_0''' + f_0 F_0'' + f_0' F_0 - (4f_0' - \gamma) F_0' = 0 \quad (18)$$

$$\frac{1}{Pr} G_0'' + f_0 G_0' + \theta_0' F_0 - f_0' G_0 - \theta_0 F_0' + G(Q + \gamma - f_0') = 0 \quad (19)$$

together with the new boundary conditions

$$\begin{aligned} F_0(0) = 0, \quad F_0'(0) = 0, \quad G_0(0) = 0 \\ F_0'(\tau) \rightarrow 0, \quad G_0(\tau) \rightarrow 0 \quad \text{as} \quad \eta \rightarrow \infty \end{aligned} \quad (20)$$

To be noted, the stability of the steady flow solutions are determined by the smallest eigenvalue  $\gamma$ . Then, to determined the possible range of eigenvalues, we relax a boundary condition on  $F_0(\eta)$  or  $G_0(\eta)$  (Harris et al. (2009)). For the current investigation, we choose the boundary condition  $F'_0 \rightarrow 0$  as  $\eta \rightarrow \infty$  to be relaxed. Then, the updated boundary condition as  $F''_0(0) = 1$  will use to solved the equations (18) - (20).

## 4. Numerical method

In order to solve the boundary value problem of equations (7) and (8) subject to boundary conditions (9), the shooting method by Maple software is applied by converting it into an initial value problem. Therefore, we set

$$f' = Fp, \quad f'' = Fpp, \quad f''' = -[FFpp + 2(1 - Fp^2)], \quad (21)$$

$$\theta' = \theta p, \quad \theta'' = -Pr[F\theta p - Fp\theta + Q\theta], \quad (22)$$

with the boundary conditions

$$\begin{aligned} F(0) = s, \quad Fp(0) = \lambda, \quad Fpp(0) = \alpha \\ \theta(0) = 1, \quad \theta p(0) = \beta. \end{aligned} \quad (23)$$

Firstly, we assume an initial value for  $Fpp(0)$  ( $f''(0)$ ) and  $\theta p(0)$  ( $\theta'(0)$ ) in order to carry out the integration in equations (21) and (22). At the same time, the values of the parameters involved are fixed and also assumed as a suitable finite value for  $\eta \rightarrow \infty$  as  $\eta_\infty$ . Since these values are not given in the boundary conditions (23), by using trial and error, the suitable guess values for  $f''(0)$ ,  $\theta'(0)$  and  $\eta_\infty$  are made and integration is carried out. The assumed values of  $f''(0)$ ,  $\theta'(0)$  and  $\eta_\infty$  until fulfilled boundary conditions in equation (23) which are  $f'(\eta_\infty) = 1$  and  $\theta(\eta_\infty) = 0$ . This step will be repeated until it gets specific value of  $f''(0)$  and  $\theta'(0)$ . In this study, the boundary layer thickness  $\eta_\infty$  between 5 and 10 are used in the computation. Furthermore, when the other guess value for  $f''(0)$ ,  $\theta'(0)$  and  $\eta_\infty$  which also meets the boundary conditions in equation (23) detected in computation, this is indicating that dual solutions is exists. Thus, we continue this numerical computation by performing the stability analysis to determine which solution is stable between the two solutions.

## 5. Results and Discussions

We have rebuild several results for the skin friction coefficient  $f''(0)$  for Bhattacharyya and Vajravelu (2012) with  $s = Q = 0$  and Rohni et al. (2013)

with  $s = 0.2$  and  $Q = 0$  in order to validate our numerical results. As we can see in Figure 2, the turning (critical) point in the case of  $s = Q = 0$  as reported by Bhattacharyya and Vajravelu (2012) is  $\lambda_c = -1.487068$  and stopped at  $\lambda = -0.9734$ . Also, the turning point in the case of  $s = 0.2$  and  $Q = 0$  as reported by Rohni *et al.* (2013) is  $\lambda_c = -1.58317$  and stopped at  $\lambda = -0.95$ . In addition, comparison results Bachok *et al.* (2012) for the case of stretching sheet ( $\lambda > 0$ ) is shown in Table 1. All the comparisons have a number of similarities and therefore, this result has further strengthened our confidence for us to continue further.

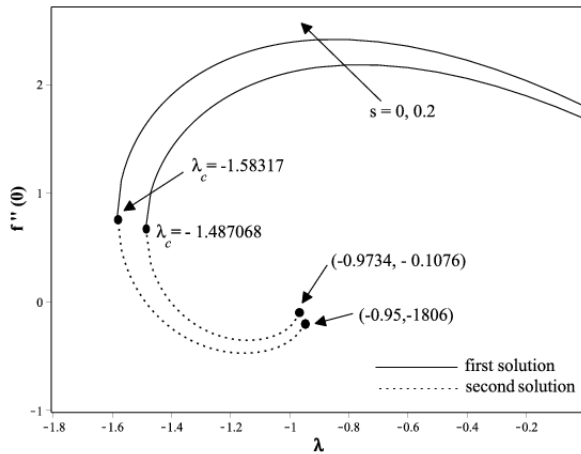


Figure 2: Variation of  $f''(0)$  for  $s = 0$  and  $s = 0.2$

Table 1: Comparison values of  $f''(0)$  and  $-\theta'(0)$  for  $s = Q = 0$  with  $Pr = 6.2$

$\lambda$	Present Study		Bachok <i>et al.</i> (2012)	
	$f''(0)$	$-\theta'(0)$	$f''(0)$	$-\theta'(0)$
-0.5	2.11817	0.68700	2.1882	0.6870
0	1.68722	1.71477	1.6872	1.7148
0.5	0.96042	2.48742	0.9604	2.4874

Table 2 shows the numerical results of the Nusselt number  $-\theta'(0)$  with and without the presence of suction and heat generation parameter. Here, we take the value of the shrinking parameter  $\lambda = -1.48$ . Our interest is to examine the influences of heat generation towards the heat transfer when the suction parameter is absent or added. Interestingly, the skin friction coefficient have a constant value for both solutions when increasing the heat generation

parameter as it comes to no surprise since that the heat generation parameter is absent in equation (9). Thus, Figure 3 displays this situation which fixes the value of suction as  $s = 1$ .

Table 2: The values of  $-\theta'(0)$  for some values of  $s$  and  $Q$  with  $\lambda = -1.48$  and  $Pr = 1$

$s$	$Q$	$-\theta'(0)$	
		First Solution	Second Solution
0	0	-0.53827	-0.82112
	0.5	-1.38607	-2.01999
	1	-0.3943	-8.76319
0.5	0	0.23539	-2.15847
	0.5	-0.22324	-13.82547
	1	-0.96541	4.29536
1	0	0.78821	-4.57391
	0.5	0.45141	11.49116
	1	-0.00391	2.76877

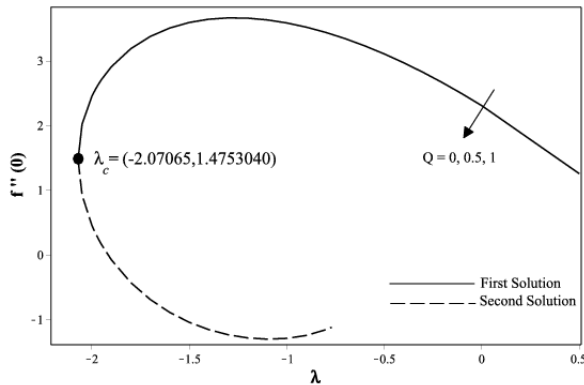


Figure 3: Variation of  $f''(0)$  for some values of  $Q$  with  $s = 1$  and  $Pr = 1$

It is apparent from Figure 4 that, as the heat generation increases with the presence or without of suction, the rate of heat transfer is decreases. Furthermore, the transfer rate of heat increases as suction parameter increases but decrement with increasing of heat generation parameter. For that reason, the increment of suction parameter leads to accelerate the transverse fluid motion as well as to lead it to a higher heat transfer rate. It is supported by looking at Figure 5 which is increasing the suction parameter, the heat transfer rate is increasing but decreasing with heat generation parameter. All of these

conditions refer to the numerical results of the first solution. There were no significant for the second solution since it is not stable

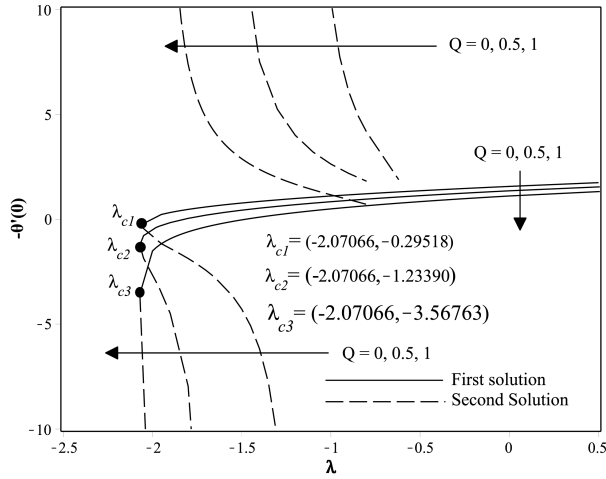


Figure 4: Variations of  $-\theta'(0)$  for some values of  $Q$  with  $s = 1$  and  $Pr = 1$

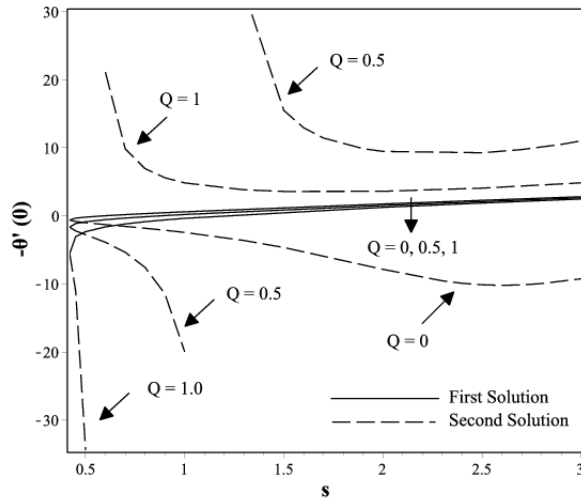


Figure 5: Variations of  $-\theta'(0)$  for some values of  $s$  with  $Q = 0, 0.5, 1$  and  $Pr = 1$

Figure 6 illustrates the effect of the Prandtl number  $Pr$  on temperature profiles. It is seen that the temperature gradient at the surface increases as  $Pr$  increases. Thus, the local Nusselt number  $-\theta'(0)$ , which represents the heat transfer rate at the surface increases (in absolute sense) as the Prandtl number  $Pr$  increases. The velocity profiles  $f'(\eta)$  and temperature profiles  $\theta'(\eta)$  for the first and second solutions but with a different shape are illustrated in Figures 7 and 8. Both profiles are considered as the case for the fixed values of  $s = Q = 1$  but with different values of  $\lambda$ . In Figure 7, there is a clear trend of decreasing the velocity when the magnitude of  $\lambda$  is increased for the first solution while the velocity is increased in the case of the second solution. However, it is contrary with the pattern of the temperature profiles in which temperature is increasing with an increase of the magnitude of  $\lambda$  in the first solution, while it is decreasing for the second solution. In addition, the thickness of boundary layer demonstrates a thinner for the first solution than the second solution for both profiles.

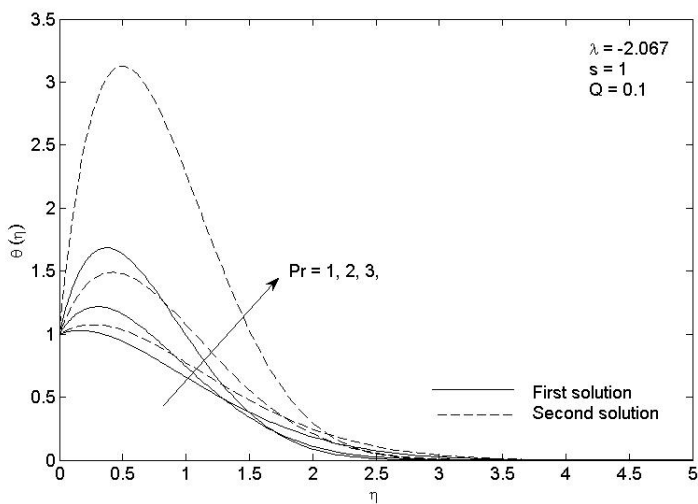


Figure 6: Temperature profiles for some values of  $Pr$

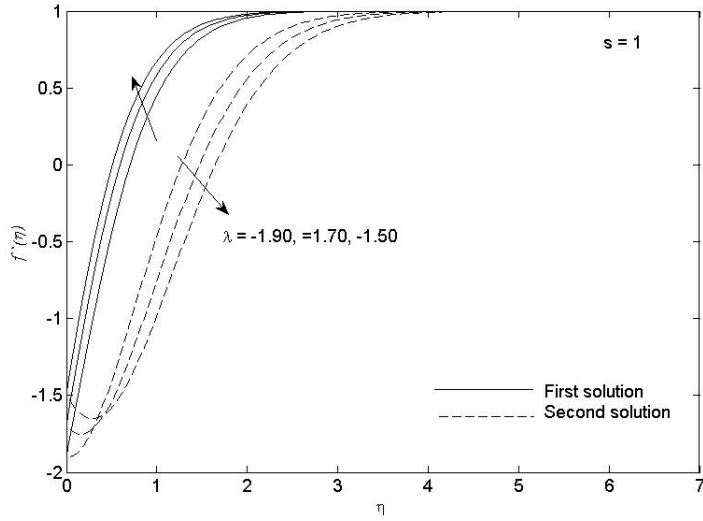


Figure 7: Velocity profiles for some values of  $\lambda$

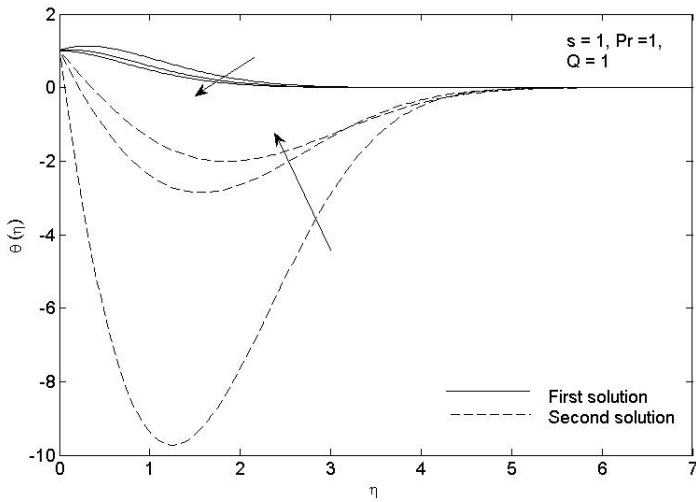


Figure 8: Temperature profiles for some values of  $\lambda$

Based on the findings of the numerical results, there are non-unique solutions exist. Therefore, we continue to perform the stability analysis. Table 3 lists the value of smallest eigenvalues  $\gamma$  for both the first and second solutions at several values of  $\lambda$  when  $s = Q = 0, 0.5, 1$ . Considerable progress have been made, only the first solutions are physically significant and valuable.

Table 3: Smallest eigenvalues of  $\gamma$  for selected values of  $\lambda$  when  $Pr = 1$

$s$	$Q$	$\lambda$	First solution	Second solution
0	0	-1.48	0.4202	-0.4168
		-1.46	0.8228	-0.8097
		-1.44	0.3943	-0.3913
0.5	0	-1.74	0.3943	-0.3913
		-1.70	1.0787	-1.0561
		-1.65	1.5527	-1.5049
1	0	-2.00	1.3523	-1.3188
		-1.95	1.7627	-1.7049
		-1.70	3.0310	-2.8431
1	0.5	-1.98	1.5304	-1.4873
		-1.85	2.3673	-2.2594
		-1.70	3.0310	-2.8431
1	1	-1.97	1.6118	-1.5638
		-1.87	2.2609	-2.1631
		-1.77	2.7459	-2.5961

## 6. Conclusions

The current study was designed to determined the influences of heat generation and suction towards fluid flow at stagnation-point and the transfer rate of heat over an exponentially shrinking sheet. Our findings would seem to conclude that, the increasing of suction parameter contribute the increasing of heat transfer rate. In other hand, increasing the heat generation parameter tend to the decreasing of heat transfer rate. In addition, the stability analysis was performed in this study to identify which of the dual solutions is stable and unstable. We have obtained comprehensive results proving that only the first solution is stable and acceptable in fluid flow.

## References

- Animasaun, I., Adebile, E., and Fagbade, A. (2016). Casson fluid flow with variable thermo-physical property along exponentially stretching sheet with suction and exponentially decaying internal heat generation using the homotopy analysis method. *Journal of the Nigerian Mathematical Society*, 35(1):1–17.
- Awaludin, I., Weidman, P., and Ishak, A. (2016). Stability analysis of stagnation-point flow over a stretching/shrinking sheet. *AIP Advances*, 6(4):045308.
- Bachok, N., Ishak, A., and Pop, I. (2012). Boundary layer stagnation-point flow and heat transfer over an exponentially stretching/shrinking sheet in a nanofluid. *International Journal of Heat and Mass Transfer*, 55:8122–8128.
- Bhattacharyya, K. (2011). Boundary layer flow and heat transfer over an exponentially shrinking sheet. *Chinese Physics Letters*, 28:074701.
- Bhattacharyya, K. and Vajravelu, K. (2012). Stagnation-point flow and heat transfer over an exponentially shrinking sheet. *Communications in Nonlinear Science and Numerical Simulation*, 17:2728–2734.
- Bhatti, M. and Rashidi, M. (2016). Effects of thermo-diffusion and thermal radiation on williamson nanofluid over a porous shrinking/stretching sheet. *Journal of Molecular Liquids*, 221:567–573.
- El-Bashbeshy, E.-S., Emam, T. G., and Abdel-Wahed, M. S. (2015). The effect of thermal radiation, heat generation and suction/injection on the mechanical properties of unsteady continuous moving cylinder in a nanofluid. *Thermal science*, 19:1591–1601.
- Elbashbeshy, E. and Bazid, M. (2004). Heat transfer in a porous medium over a stretching surface with internal heat generation and suction or injection. *Applied mathematics and computation*, 158:799–807.
- Fang, T. (2008). Boundary layer flow over a shrinking sheet with power-law velocity. *International Journal of Heat and Mass Transfer*, 51:5838–5843.
- Fang, T. and Zhang, J. (2009). Closed-form exact solutions of mhd viscous flow over a shrinking sheet. *Communications in Nonlinear Science and Numerical Simulation*, 14:2853–2857.
- Gireesha, B., Mahanthesh, B., Gorla, R. S. R., and Manjunatha, P. (2016). Thermal radiation and hall effects on boundary layer flow past a non-isothermal stretching surface embedded in porous medium with non-uniform

- heat source/sink and fluid-particle suspension. *Heat and Mass Transfer*, 52(4):897–911.
- Hafidzuddin, E. H., Nazar, R., Arifin, N., and Pop, I. (2015). Stability analysis of unsteady three-dimensional viscous flow over a permeable stretching/shrinking surface. *Journal of Quality Measurement and Analysis*.
- Harris, S., Ingham, D., and Pop, I. (2009). Mixed convection boundary-layer flow near the stagnation point on a vertical surface in a porous medium: Brinkman model with slip. *Transport in Porous Media*, 77:267–285.
- Hsiao, K.-L. (2016). Stagnation electrical mhd nanofluid mixed convection with slip boundary on a stretching sheet. *Applied Thermal Engineering*, 98:850–861.
- Ishak, A. (2014). Flow and heat transfer over a shrinking sheet: A stability analysis. *International Journal of Mechanical, Aerospace, Industrial and Mechatronics Engineering*, 8:905–9.
- Jahan, S., Sakidin, H., Nazar, R., and Pop, I. (2017). Flow and heat transfer past a permeable nonlinearly stretching/shrinking sheet in a nanofluid: A revised model with stability analysis. *Journal of Molecular Liquids*, 233:211–221.
- Khan, Z., Qasim, M., Haq, R. U., and Al-Mdallal, Q. M. (2017). Closed form dual nature solutions of fluid flow and heat transfer over a stretching/shrinking sheet in a porous medium. *Chinese Journal of Physics*, 55(4):1284–1293.
- Mahapatra, T. R. and Nandy, S. (2011). Stability analysis of dual solutions in stagnation-point flow and heat transfer over a power-law shrinking surface. *International Journal of Nonlinear Science*, 12:86–94.
- Mahapatra, T. R., Nandy, S. K., and Gupta, A. S. (2010). Dual solution of mhd stagnation-point flow towards a stretching surface. *Engineering*, 2:299.
- Malvandi, A., Hedayati, F., and Domairry, G. (2013). Stagnation point flow of a nanofluid toward an exponentially stretching sheet with nonuniform heat generation/absorption. *Journal of Thermodynamics*, 2013.
- Merkin, J. (1986). On dual solutions occurring in mixed convection in a porous medium. *Journal of engineering Mathematics*, 20:171–179.
- Miklavcic, M. and Wang, C. (2006). Viscous flow due to a shrinking sheet. *Quarterly of Applied Mathematics*, 64:283–290.

- Molla, M. M., Hossain, M. A., and Paul, M. C. (2006). Natural convection flow from an isothermal horizontal circular cylinder in presence of heat generation. *International Journal of Engineering Science*, 44:949–958.
- Nandy, S. K. and Mahapatra, T. R. (2013). Effects of slip and heat generation/absorption on mhd stagnation flow of nanofluid past a stretching/shrinking surface with convective boundary conditions. *International Journal of Heat and Mass Transfer*, 64:1091–1100.
- Naveed, M., Abbas, Z., Sajid, M., and Hasnain, J. (2017). Dual solutions in hydromagnetic viscous fluid flow past a shrinking curved surface. *Arabian Journal for Science and Engineering*, pages 1–6.
- Rashad, A., Rashidi, M., Lorenzini, G., Ahmed, S. E., and Aly, A. M. (2017). Magnetic field and internal heat generation effects on the free convection in a rectangular cavity filled with a porous medium saturated with cu–water nanofluid. *International Journal of Heat and Mass Transfer*, 104:878–889.
- Rohni, A. M., Ahmad, S., Ismail, A. I. M., and Pop, I. (2013). Boundary layer flow and heat transfer over an exponentially shrinking vertical sheet with suction. *International Journal of Thermal Sciences*, 64:264–272.
- Roşca, A. V. and Pop, I. (2013). Flow and heat transfer over a vertical permeable stretching/shrinking sheet with a second order slip. *International Journal of Heat and Mass Transfer*, 60:355–364.
- Saleh, S. H. M., Arifin, N. M., Nazar, R., Ali, F. M., and Pop, I. (2014). Mixed convection stagnation flow towards a vertical shrinking sheet. *International Journal of Heat and Mass Transfer*, 73:839–848.
- Sharma, R., Ishak, A., and Pop, I. (2014). Stability analysis of magnetohydrodynamic stagnation-point flow toward a stretching/shrinking sheet. *Computers & Fluids*, 102:94–98.
- Suriyakumar, P. and Devi, S. A. (2015). Effects of suction and internal heat generation on hydromagnetic mixed convective nanofluid flow over an inclined stretching plate. *European Journal of Advances in Engineering and Technology*.
- Wang, C. (2008). Stagnation flow towards a shrinking sheet. *International Journal of Non-Linear Mechanics*, 43:377–382.
- Weidman, P., Kubitschek, D., and Davis, A. (2006). The effect of transpiration on self-similar boundary layer flow over moving surfaces. *International journal of engineering science*, 44:730–737.